PHYSICSAccess Research Paper
ISSN Online: 2756-3898, ISSN Print: 2714-500X https://doi.org/10.47514/phyaccess.2024.4.2.007

First Principle Study of Structural, Electronic, Mechanical and Optical Properties of Bulk Niobium Dichalcogenide NbX_2 (X=S, SE) within a Visible Phonon Energy Range

Jabir A Tahir[1, 2], Godwin J Ibeh[2] and Alhassan Shuaibu[1]

[1] Department of Physics, Kaduna State University, Kaduna PMB 2339, Kaduna, Nigeria
[2] Department of Physics, Nigerian Defence Academy, Kaduna, Nigeria

Corresponding E-mail: jabiradamutahir@gmail.com

Received 31-07-2024
Accepted for publication 12-09-2024
Published 20-09-2024

Abstract

An intensive study on structural, electronic mechanical and optical properties of bulk Niobium Dichalcogenides NbX_2 (X=S, Se) was carried out using the first principle. The structural parameters such as Equilibrium Lattice Parameters, Volume, Bulk Modulus, and First-Derivative Modulus were calculated to determine if the materials are energetically stable. Elastic constants were further obtained from which mechanical properties i.e. bulk, Young's and shear moduli and consequently Poisson's ratio were obtained. Based on the well-known Born stability conditions Bulk-NbS_2 is most likely mechanically anisotropic ductile material. While Bulk-$NbSe_2$ for the predicted B/G ratio in all three methods is less than a critical value of 1.75, hence this shows that $NbSe_2$ is a brittle material exploring its electronic and optical properties whose motivation was to find out the most stable phase and ascertain if these materials could be used in various fields that suit their mechanical and optical properties. Furthermore, from the calculated optical spectra, plasma frequencies were analyzed which indicated the possibility of applying the material in plasmonic-related fields.

Keywords: Niobium Dichalcogenides; Density functional theory plus Hubbard (DFT+U); dependent density functional theory (TDDFT), electronic and optical properties.

I. Introduction

Niobium dichalcogenides with the general formula NbX_2 (X= S, Se and Te) have recently become the most interesting materials in many technological applications. Among them, a bulk-NbS_2 has been experimentally synthesized by creating stoichiometric samples from the elements by reacting them at 950 °C and then quenching them at 750 °C for annealing [1]. During annealing, the products' stoichiometry depended on the pressure of excess Sulphur. For $Nb_{1+x}S_2$, only two phases were found in the range of $0<x<0.18$ a non-stoichiometric phase corresponding to 3R-$Nb_{1+x}S_2$ and a stoichiometric line phase corresponding to the 2H polytypes NbS_2. There was only the 3R polytypes for $0.07 < x < 0.18$ [2-3]. Meissner flux expulsion measurements of superconducting transition temperatures revealed that 2HNbS_2 superconducts at 6.3 K. Above 1.7 K, 3R-$Nb_{1+x}S_2$ does not superconduct [4]. They observed that 2H-NbS_2 had a minor linear rise in susceptibility with decreasing temperature and was nearly twice as great. The authors observed the presence of the

distinct phases in niobium disulphide, which are categorized as stoichiometric (2H-NbS_2 and 3R-$Nb_{1+x}S_2$) and non-stoichiometric (2H-$Nb_{1+x}S_2$ and 3R-Nb1+xS_2). They postulated that the surplus niobium atoms in the space between the sandwiches allowed nonstoichiometric behaviour [5].

$NbSe_2$ is reported to crystallize in the P6/mmc space group by Kershaw et al. [6]. To create single crystals, the chemical transport method employed either bromine or iodine as the transport agent. They used a Norelco diffractometer and monochromatic light (AMR-202 Focusing monochromator) to determine the crystallographic properties of $NbSe_2$ on powder samples. Based on their resistivity curves, $NbSe_2$ exhibited metallic characteristics. As measured on single crystals, the superconducting transition for $NbSe_2$ occurred at 7 K, consistent with the value reported [7, 8]. $NbSe_2$ functions like a metal because the conduction band has a free electron [9]. The 2H-$NbSe_2$ ABA stacking sequence. The comparatively weak van der Waals interaction between neighbouring chalcogenide layers in $NbSe_2$ and other TMDs causes mechanical and electronic anisotropy, and this bonding allows bases to intercalate [11, 12]. As 2H-$NbSe_2$ temperatures rise, the sign of the Hall coefficient shifts from n-type to p-type at 26 K, [7, 13]. This behaviour was indeed unusual in that, at room temperature, the Hall coefficient had a positive sign while, the Seebeck coefficient had a negative sign when the hydrostatic pressure of 17 kbar was applied, the superconducting transition temperature of the layer crystal niobium diselenide increased from 6.9 K to 8.5 K.

Looking at the progress on the above materials' further investigations into their properties such as electronic and optical can make them be used in many technological applications. Density functional theory (DFT) has recently become one of the most successful tools in predicting and analyzing such mentioned properties, and the obtained DFT results were reported to be close to experimental results in similar transition metal dichalcogenides [14-16]. Recently many DFT investigations on the monolayer and bilayer of NbX_2 (X=S, Se) have been reported [17-20] and in each case, different results which are a little far from the reported experimental ones have been obtained recommending that a bulk of such materials need to be investigated in details. Hence, this work used the DFT plus Hubbard (DFT+U) function [21] to study the structural, electronic properties of the bulk NbX_2 (X=S, Se) and further used time-dependent density functional theory (TDDFT) and to examine the optical property within the visible photon energy range.

II. COMPUTATIONAL METHOD

Using density functional theory (DFT) as implemented in the Quantum ESPRESSO package [22] all calculations were carried out and a converged cutoff energy of 500 eV was set during optimization and electronic properties calculation. A special k-point of $6 \times 6 \times 1$ grid meshes signified by Monkhorst-Pack [23] was set off. The convergence of energy and force are set to 1×10^{-6} eV and 0.01 eV/Å, respectively. For the geometry optimizations and electronic properties calculations, we have used a Perdew-Burke-Ernzerhof (PBE) [24] functional within the generalized gradient approximation (GGA) [25]. To get more accurate electronic properties, we adopt the GGA+U method with U = 4 eV for the 4d electrons of the Nb atom.

The optical properties of crystalline materials are mostly calculated using the imaginary $\varepsilon_2(\omega)$ and real $\varepsilon_1(\omega)$ component of the complex dielectric function $\varepsilon(\omega)$ given by (12).

$$\varepsilon(\omega = \varepsilon_1(\omega) + i\varepsilon_2(\omega) \quad (1)$$

The imaginary part can be calculated from the Kubo-Greenwood equation expressed as

$$\varepsilon_2(\omega) = \frac{2\pi e^2}{\Omega \varepsilon_o} \sum_{k,v,c} |\langle \Psi_k^c | u.r | \Psi_k^v \rangle|^2 \, \delta(E_k^c - E_k^v - E) \quad (2)$$

Moreover, the real part $\varepsilon_1(\omega)$ of the dielectric function can be determine from the imaginary component using Kramer-Kronig equation.

$$\varepsilon_1(\omega) = 1 + \left(\frac{2}{\pi}\right) \int_0^\infty d\omega \quad (3)$$

$$\alpha(\omega) = \sqrt{2}\omega \left[\sqrt{\{\varepsilon_1(\omega)\}^2 + \{\varepsilon_2(\omega)\}^2} - \varepsilon_1(\omega)\right]^{\frac{1}{2}} \quad (4)$$

$$\sigma(\omega) = \frac{\omega \varepsilon_2(\omega)}{4\pi} \quad (5)$$

$$n = \sqrt{\left(\frac{\sqrt{\{\varepsilon_1(\omega)\}^2 + \{\varepsilon_2(\omega)\}^2} + \varepsilon_1(\omega)}{2}\right)} \quad (6)$$

In the above equation, ω is the frequency of the phonon, Ω is the unit cell volume, u is the unit vector, and e is the charge of the electron also Ψ_k^c and Ψ_k^v are wavefunctions for conduction and valence band electrons respectively at k. $\alpha(\omega)$is the absorption coefficient, $\sigma(\omega)$ optical conductivity and n is the refractive index of the material.

III. RESULTS AND DISCUSSION

A. Structural properties of Bulk NbX2 (X=S, Se)

The optimized crystal structure of both Bulk NbS_2 and Bulk $NbSe_2$ is given in Fig. 1, the two materials have a hexagonal crystal structure space group (P63/mmc), starting with NbS_2 bulk as depicted in Fig. 1 (a) which forms a layered compound with the P3m1 space group. The interlayer stacking of the compound possesses Nb metal atoms inserted between sulphur atoms having a nonmetal character with strong covalent bonds involved in the association of the sulphur metal. Similarly, the bulk $NbSe_2$ has the same form only with the Nb metal atoms inserted between selenium atoms as shown in Fig. 1 (b), it is only mildly influenced by van der Waals forces. This is in excellent agreement with the reported results [26-28].

To determine the structural stability, we have calculated the total energies for both bulk NbS_2 and $NbSe_2$. The obtained results are summarized in Table I. The calculated total energies are -210.1078 and -223.3221 Ry for NbS_2 and $NbSe_2$

respectively. These values indicate that these materials are thermodynamically stable due to the negative sign [29].

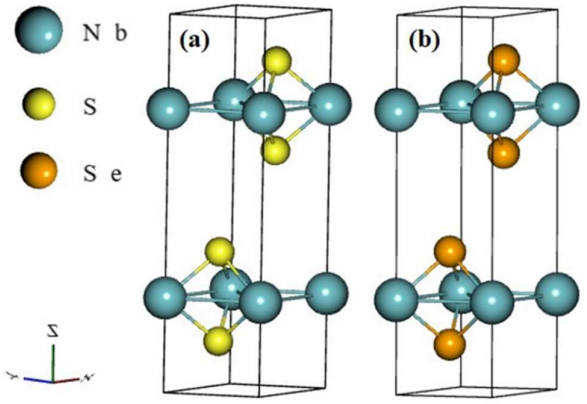

Fig. 1. Optimized crystal structure of (a) Bulk NbS_2 (b) Bulk $NbSe_2$ with optimized GGA parameters.

Similarly, other structural parameters such as Equilibrium Lattice Parameters, Volume, Bulk Modulus, and First-Derivative Modulus were calculated using (7).

$$E_{tot}(a) = E_o + \frac{9V_oB_o}{16}\left\{\left[\left(\frac{a_o}{a}\right)^2 - 1\right]^3 B_o' + \left[\left(\frac{a_o}{a}\right)^2 - 1\right]^2 \left[6 + 4\left(\frac{a_o}{a}\right)^2\right]\right\} \quad (7)$$

Where a_o equilibrium lattice is constant, V_o is the equilibrium volume per atom, B_o is the bulk modulus at zero pressure and the pressure derivative of the bulk modulus $B_o' = \left(\frac{\partial B}{\partial P}\right)_T$.

The results summarized in Table I, show that the two systems are more stable in a possible magnetic state. This finding agrees with the results reported in [30-32].

Table I. Calculated Equilibrium Lattice Parameters, Volume, Bulk Modulus, and Their First-Derivative Modulus of Bulk NbX_2 (X=S, Se).

Structure	*a* (Å)	*c* (Å)	*V* (Å^3)	B_0	*B'*
Bulk NbS_2	3.32	12.43	122.09	144.1	5.96
	3.37[a]	12.62[a]	124.08	144.8[a]	5.23[a]
	3.23[b]	12.56[b]	119.46	141.5[c]	5.65[c]
	3.17[c]	12.32[c]	107.18		
Bulk $NbSe_2$	3.55	13.48	147.43	166.4	7.49
	3.50[c]	13.41[c]	142.23	164.8	7.23
	3.45[c]	13.65[c]	150.42	167.7	7.55
	3.48[a]	13.72[a]	149.42		

[a][31] [b][30] [c][32]

B. Electronic properties of Bulk NbX_2 (X=S, Se)

Using the above-optimized parameters the electronic band structures and corresponding atomic density of state (ADOS) of the two bulk systems (NbS_2 and $NbSe_2$) were obtained and depicted in Fig. 2 and 3 respectively. From Fig. 2(a), it was observed that the valence band of bulk NbS_2 crossed the Fermi level at the M-high symmetry point, indicating a semi-metallic or semi-conductor character. These results agree with studies reported in [30-32]. Fig 2. (b) shows the atomic density of states of the NbS_2. The Total DOS affirmed the semi-metallic character as seen in the band structure, a high peak near the Fermi level has been observed and a possible small magnetic moment of Nb atom is indicated. In both cases, contributions to the electronic states come mainly from the S atom p-type orbitals and the metal atom d-type orbitals.

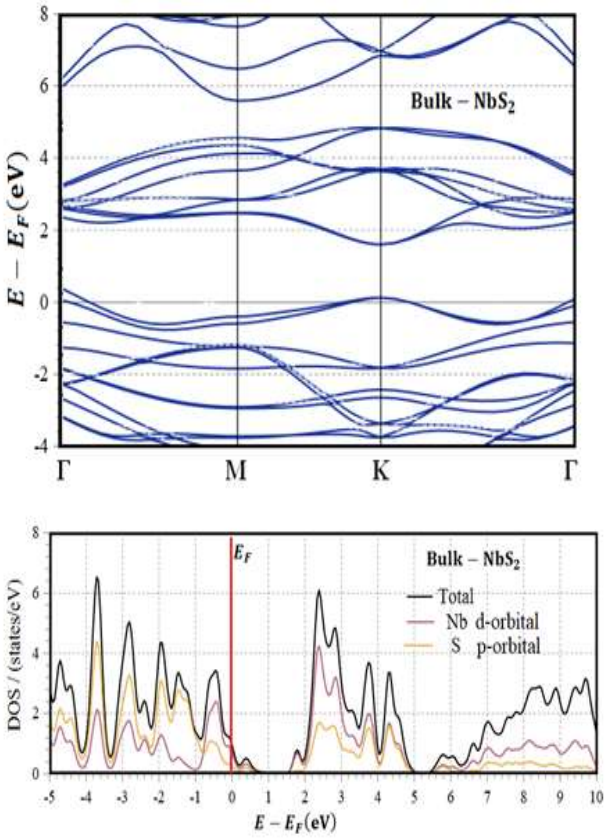

Fig. 2. Calculated (a) electronic band structure and (b) atomic density of state of Bulk NbS_2 using DFT-GGA optimized parameters.

Similarly, when considering the calculated electronic band structure and corresponding DOS of Bulk $NbSe_2$ Fig. 3(a and b). It proves the semi-metallic nature observed in NbS_2, only with number bands in both CB and VB as seen in Fig. 3(a). This semi-metallic character is also revealed in DOS plot Fig. 3(b), which shows a highly localized state cutting through the Fermi level. The DOS analysis reveals the electronic state at the Fermi level primarily comes from Nb d and Se p orbitals which hybridized nearly in the entire energy range, indicating a strong covalency between these two atoms. These results are in excellent agreement with studies reported in [30], [31] and [32].

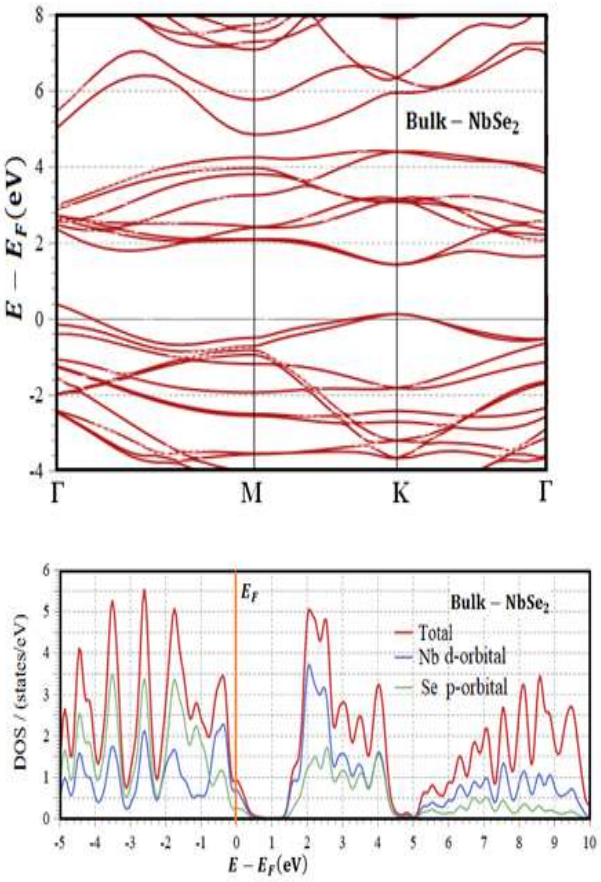

Fig. 3. Calculated (a) electronic band structure and (b) atomic density of state of Bulk $NbSe_2$ using DFT-GGA optimized parameters.

C. *Mechanical Properties*

Analysis of elastic constants (C_{ij}) is essential for understanding the mechanical properties of the materials. These constants can be calculated for anisotropic materials by solving the compliance matrix given by

$$C_{ij} = \begin{pmatrix} C_{11} & C_{12} & C_{13} & C_{14} & C_{15} & C_{16} \\ & C_{22} & C_{23} & C_{24} & C_{25} & C_{26} \\ & & C_{33} & C_{34} & C_{35} & C_{36} \\ & & & C_{44} & C_{45} & C_{46} \\ & & & & C_{55} & C_{56} \\ & & & & & C_{66} \end{pmatrix} \quad (8)$$

These constants vary from one crystal system to another based on the respective point groups and Born stability conditions [136, 156]. For The materials which are Hexagonal with a point group of 6mm, the mechanical stability criteria are

$$C_{11} > |C_{12}|., C_{44} > 0., C_{66} > 0., 2C_{13}^2 < (C_{11} + C_{12}) \quad (9)$$

Similarly, for the bulk and shear moduli these constants are related within Voight, Reuss and Hill Averaging schemes by the following expressions.

1) Voight Average schemes

$$B_V = \frac{2}{9}\left[C_{11} + C_{12} + 2C_{13} + \frac{1}{2}C_{33}\right] \quad (10)$$

$$G_V = \frac{1}{30}[C_{11} + C_{12} + 2C_{33} - 4C_{13} + 12C_{55} + 12C_{66}] \quad (11)$$

2) Reuss Average schemes

$$B_R = \frac{[5C_{55}C_{66}(C_{11}+4C_{12})C_{33} - 2C_{12}^2]}{C_{11}+C_{12}+2C_{33}-4C_{12}} \quad (12)$$

$$G_R = \frac{[5C_{55}C_{66}(C_{11}+4C_{12})C_{33} - 2C_{12}^2]}{2\{3B_V C_{55}C_{66} + [(C_{11}+4C_{12})C_{33} - 2C_{12}^2](C_{55}+C_{66})\}} \quad (13)$$

3) Hill Average schemes

$$B_H = \frac{1}{2}(B_V + B_R) \quad (14)$$

$$G_H = \frac{1}{2}(G_V + G_R) \quad (15)$$

Thermo_pw code of QE was used to obtain the numerical value of the above for both Bulk NbS_2 and Bulk $NbSe_2$ and summarized in Tables II and III respectively.

Table II. Calculated independent elastic coefficients for Bulk NbS_2 and $NbSe_2$

Materials	C11	C12	C13	C33	C44
Bulk-NbS_2	140.870	46.031	1.655	43.391	4.555
Bulk-$NbSe_2$	152.040	48.184	14.207	16.545	15.588

From Table II it is seen that the Born stability conditions have been achieved for the two bulk materials, hence we can affirm that Bulk NbS_2 and $NbSe_2$ are mechanically stable, although we did not compare The results with other calculated values recently Azizi et al [30] confirmed experimentally both NbS_2 and $NbSe_2$ are mechanically stable.

Table III. Calculated B, E, G, ν and B/G for Bulk NbS_2 and $NbSe_2$

Material	Method	B	E	G	ν	B/G
Bulk-NbS_2	Voight (V)	45.708	72.511	30.075	0.2155	1.5198
	Reuss (R)	30.021	25.202	10.027	0.3216	2.9940
	Hill (H)	37.8645	50.513	20.051	0.2616	1.8884
Bulk-$NbSe_2$	Voight (V)	51.811	81.305	32.008	0.2157	1.6186
	Reuss (R)	16.367	40.113	18.198	0.0952	0.8993
	Hill (H)	42.2725	62.011	25.103	0.2011	1.6839

From Table III, for Bulk-NbS_2 the three averaging schemes gave B/G values ranging between 1.52 and 2.99. This indicates that Bulk-NbS_2 is most likely mechanically anisotropic ductile material. For Bulk-$NbSe_2$ the predicted B/G ratio in all three methods is less than a critical value of 1.75, hence this shows that $NbSe_2$ is a brittle material. These results agree with theoretical and experimental reports in [30-32].

D. Optical properties of Bulk NbX_2 (X=S, Se)

1) Calculated optical properties of Bulk- NbS_2

The material's optical properties make its behaviour in the presence of electromagnetic radiation more understandable. When determining the dielectric properties of a compound with hexagonal symmetry, the electric vector E might be either parallel or perpendicular to the z-axis. Using the Sternwheeler approach within the time-dependent density functional theory (TDDFT) as implemented in the Thermo_pw code of the Quantum ESPRESSO, the complex dielectric constant of Bulk NbS_2 has been calculated. The obtained real $\varepsilon_1(\omega)$and imaginary $\varepsilon_2(\omega)$part of the dielectric function is given in the energy range of 0-10 eV as given in Fig. 4(a, b) from the plot it can be seen that both $\varepsilon_1(\omega)$ and $\varepsilon_2(\omega)$ have similar characters in the case of the x and y axis but different z direction, which results in identical optical functions in the x and y axis since all other optical properties are functions of $\varepsilon(\omega) = \varepsilon_1(\omega) + i\,\varepsilon_2(\omega)$.

Fig. 5(a-f) gives the calculated optical properties such as absorption coefficient, reflectivity, refractive index, extinction coefficient, Absorption coefficient within the visible range and Reflectivity within the visible range of bulk-$NbSe_2$. The plot shows no distinct pattern in the refractive index in Fig. 5(c) and extinction coefficient in Fig. 5(d). Considering the visible regime, maximum absorption along the z-axis occurs between the photon range of 1.80-p.

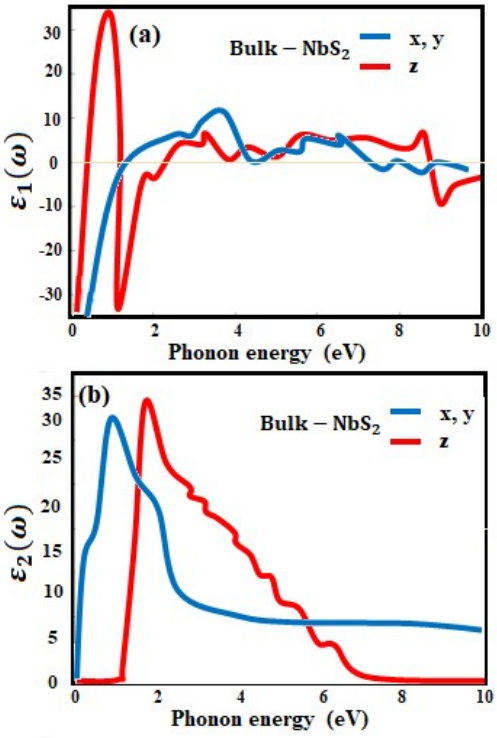

Fig. 4. Calculated real and imaginary parts of the complex dielectric function of bulk-$NbSe_2$

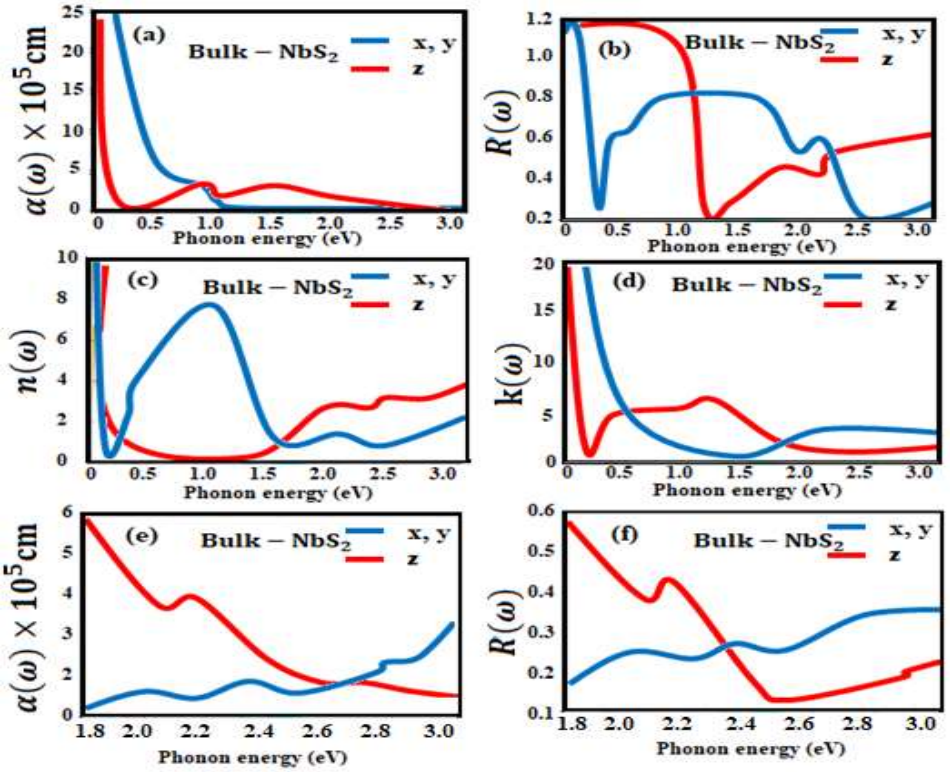

Fig. 5. (a) absorption coefficient, (b) reflectivity, (c) refractive index, (d) extinction coefficient, Absorption (e) coefficient within the visible range and Reflectivity within the visible range of the bulk-NbS_2.

Also, within the visible range, wide absorption peaks occur at around 2.00 eV and 2.46 eV for the z-axis and x, and y-axis respectively. This implies that when the incoming photon hits bulk-NbS_2 along the x and y axis, it will appear orange in colour whereas when it strikes along the z-axis, it will appear green in colour. The screened in-plane plasma frequencies occur at around 1.2 eV, 3.6 eV, 3,8 eV, 5.0 eV and 9.0 eV whereas out-of-plane plasma frequencies occur at around 0.3 eV, 1.2 eV, 2.2 eV and 9.0 eV as shown in Fig. 4. From the predicted values of plasma frequencies, NbS_2 is a promising plasmonic material since Plasmon excitations occur in the visible and UV region giving high Plasmon quality.

2) Calculated optical properties of Bulk- $NbSe_2$

$NbSe_2$ possesses similar optical properties to those of NbS_2. Fig. 6(a-f) gives The calculated optical properties for the bulk-$NbSe_2$, showing the magnitude of the obtained absorption coefficient along the x, y-axis (corresponding to in-plane) which exceeds along that of z-plane (corresponding to out-of-plane) up to 0.4 eV beyond the out-of-plane dominates. Intensity of in-plane reflectivity exceeds out-of-plane reflectivity up to 0.75 eV beyond which out-of-plane reflectivity exceeds in-plane reflectivity. In-plane refractive index and in-plane extinction coefficient exceed corresponding out-of-plane counterparts up to around 1.25 eV and 0.2 eV respectively beyond which out-of-plane refractive index and extinction coefficient dominate.

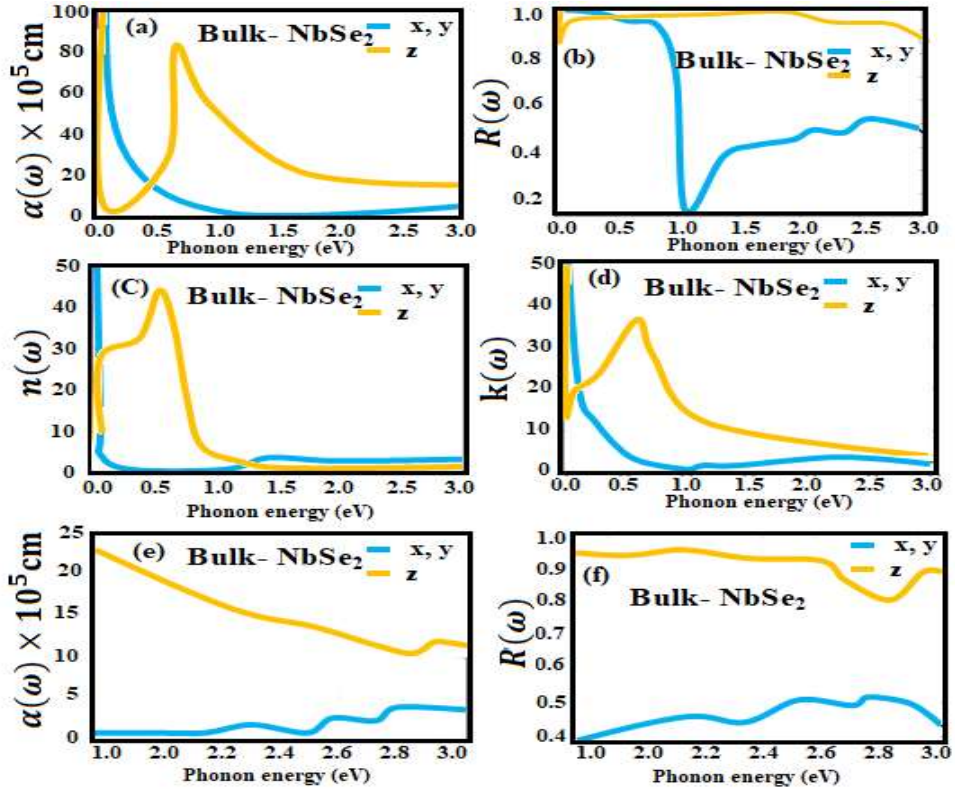

Fig. 6. (a) absorption coefficient, (b) reflectivity, (c) refractive index, (d) extinction coefficient, Absorption (e) coefficient within the visible range and Reflectivity within the visible range of the bulk-$NbSe_2$.

Within the visible range, along the z-axis (corresponding to out-plane) absorption and reflectivity exceed along the x, y-axis (corresponding to in-plane). Wide absorption peaks occur at the edge of the visible region hence we predict that when $NbSe_2$ is illuminated with light, it will appear violet in colour irrespective of the interface light shines on. Screened in-plane plasma frequencies occur at around 1.0 eV, 4.4 eV and 8.5 eV whereas several out-of-plane plasma frequencies were predicted at around 6.5 eV, 6.7 eV,6.9 eV, 7.1 eV and 7.2 eV. Its screened plasma frequencies occur at the infrared and ultraviolet region as shown in Fig. 6(e and f) hence a promising material for plasmonic-related applications. The obtained results agree with studies reported in [30] and [31].

IV. Conclusion

An investigation on the structural, electronic, mechanical, and optical properties of Bulk transition metal dichalcogenides ($NbSe_2$, NbS_2) were carried out using the first principle, with the obtained structural properties comparable to the available experimental data. From the obtained mechanical properties, the bulk NbS_2 was found to be an anisotropic ductile material, while the $NbSe_2$ was predicted to be brittle. From the

electronic band structure plots, both $NbSe_2$ and NbS_2 showed metallic characters, indicating a strong possibility of band engineering via the introduction of donor impurities which can lead to obtaining a semiconducting nature that can be applied in designing optoelectronic devices. Finally, the obtained optical properties clearly show that $NbSe_2$ and NbS_2, are promising plasmonic materials in their bulk form.

Reference

[1] Z. Wang, C. Y. Cheon, M. Tripathi, G. M. Marega, Y. Zhao, H.G. Ji, M. Macha, A. Radenovic, and A. Kis, Superconducting 2D NbS_2 grown epitaxially by chemical vapour deposition. *ACS nano*, vol. *15,* no.11, pp.18403-18410. 2021.

[2] W. G., Fisher, and M. J Sienko "Stoichiometry, Structure, and physical properties of niobium disulfide" *Inorganic Chemistry*, vol. 19, no. 1, pp. 39-43, 1980.

[3] E. Garcés, O., Salas, and L. F. Magaña, "Optical absorption and reflectivity of four 2D materials: MoS_2, MoP_2, NbS_2, and NbP_2". *Frontiers in Materials*, vol. *8*, pp. 720-768, 2021.

[4] P. Kumbhakar, C. Chowde Gowda, and C. S. Tiwary, "Advance optical properties and emerging applications of 2D materials". *Frontiers in Materials*, vol. *8*, pp. 721-514, 2021.

[5] R. Kershaw, M. Vlasse, and A. Wold, "The preparation of and electrical properties of niobium selenide and tungsten selenide". *Inorganic Chemistry*, vol. *6* no. 8, pp. 1599-1602, 1967.

[6] A. Hamill, B. Heischmidt, E. Sohn, D. Shaffer, K. T. Tsai, X. Zhang, and V. S. Pribiag, "Two-fold symmetric superconductivity in few-layer $NbSe_2$". *Nature Physics*, vol. *17,* no. 8, pp. 949-954, 2021.

[7] E. Revolinsky, G. A. Spiering, and D. J. Beerntsen, "Superconductivity in the niobium-selenium system". *Journal of Physics and Chemistry of Solids*, vol. *26,* no. 6, pp. 1029-1034, 1965.

[8] L. H. Brixner, "Preparation and properties of the single crystalline AB2-type selenides and tellurides of niobium, tantalum, molybdenum and tungsten". *J. of Inorg. and Nucl. Chem.*, vol. *24,* no, 3, pp 257-263. 1962.

[9] Y. Noat, J. A. Silva-Guillén, T. Cren, V., Cherkez, C. Brun, Pons, and S. E. Canadell, "Quasiparticle spectra of 2 H-NbSe 2: Two-band superconductivity and the role of tunnelling selectivity". *Physical Review B*, vol. *92,* no. 13, pp 1345-10, 2015.

[10] M. Rajapakse, B. Karki, U. O. Abu, S. Pishgar, M. R. K., S. S. Musa, Riyadh, and J. B. Jasinski "Intercalation as a versatile tool for fabrication, property tuning, and phase transitions in 2D materials". *npj 2D Materials and Applications*, vol. *5* no. 1, pp. 30, 2021.

[11] A. Raza, J. Z. Hassan, M. Ikram, S. Ali, U., Farooq, Q. Khan, and M. Maqbool, "Advances in liquid-phase and intercalation exfoliations of transition metal dichalcogenides to produce 2D framework". *Advanced Materials Interfaces*, vol. *8,* no. 14, pp. 200-2205, 2021.

[12] A. Majumdar, D. VanGennep, J. Brisbois, D. Chareev, A. V. Sadakov, A. S. Usoltsev, and M. Abdel-Hafiez, "Interplay of charge density wave and multiband superconductivity in layered quasi-two-dimensional materials: The case of 2H-Nb S_2 and 2H-$NbSe_2$". *Phys. Rev. Mat.*, vol. *4,* no. 8, pp. 084-005 2020.

[13] M. Pisarra, C. Díaz, and F. Martín, "Theoretical study of structural and electronic properties of 2 H-phase transition metal dichalcogenides". *Phy. Rev. B*, vol. *103,* no. 19, pp 195-416. 2021.

[14] M. Adamu, S. Alhassan, S. G. Abdu, and M. M Aliyu, "Ultra-Thin 2D $MoTe_2$ for Electron Transport Material Application in Perovskite Solar Cell": A Theoretical Approach. Phy. Access, vol. 4 no. 1. Pp. 32-43 2024.

[15] A. Mohammed, A. Shu'aibu, S. G. Abdu, and M. M. Aliyu, "Two-dimensional pure and bromine doped $MoTe_2$ and WSe_2 as electron transport materials for photovoltaic application-A DFT approach". *Comp. Cond. Matt.*, vol. *37*, pp. e00-855, 2023.

[16] Y. Zang, Y. Ma, R. Peng, H. Wang, B., Huang, and Y. Dai, "Large valley-polarized state in single-layer NbX_2 (X= S, Se) Theoretical prediction". *Nano Res.*, vol. *14*, pp. 834-839, 2021.

[17] S. Kansara, S. K. Gupta, and Y. Sonvane, "Effect of strain engineering on 2D dichalcogenides transition metal: a DFT study". *Comp. Mat. Sci.*, vol. *141*, pp. 235-242 2018.

[18] H. Du, Z. Jiang, J. Zheng, X. Zhang, W. Wang, and Z. Zhang, "Theoretical study of CDW phases for bulk NbX2 (X= S and Se)". *Phys. Chem. Chem. Phy.*, vol. *26,* no. 3, pp. 2376-2386, 2024.

[19] Y. Zhou, Z. Wang, P.Yang, X., Zu, L. Yang, X. Sun, and F. Gao, "Tensile strain switched ferromagnetism in layered NbS2 and NbSe2". *Acs Nano*, vol. *6,* no. 11, pp. 9727-9736, 2012.

[20] A. Floris, I. Timrov, B. Himmetoglu, N., Marzari, S., de Gironcoli, and M. Cococcioni, "Hubbard-corrected density functional perturbation theory with ultrasoft pseudopotentials". *Phys. Rev. B*, vol. *101,* no. 6, pp. 1-16, 2020.

[21] P. Giannozzi, S. Baroni, N. Bonini, M. Calandra, R. Car, C. Cavazzoni, and R. M. Wentzcovitch, "QUANTUM ESPRESSO: a modular and open-source software project for quantum simulations of materials". *J. of Phy.: Cond. Matt.*, vol. *21,* no. 39, pp. 395-502, 2009.

[22] H. J. Monkhorst, and J. D. Pack, "Special points for Brillouin-zone integrations". *Phys. Rev. B*, vol. *13,* no. 12, pp. 51-88, 1976.

[23] J. P. Perdew, K. Burke, and M. J. P. R. L. Ernzerhof, "Perdew, burke, and ernzerhof reply". *Phys. Rev. Lett.*, vol. *80,* no. 4, pp. 891, 1998.

[24] J. P. Perdew, "Generalized gradient approximations for exchange and correlation: A look backward and forward". *Phys. B: Cond. Matt.*, vol. *172,* no. 1-2, pp. 1-6, 1991.

[25] H. Du, Z. Jiang, J. Zheng, X. Zhang, W. Wang, and Z. Zhang, Theoretical study of CDW phases for bulk NbX_2 (X= S and Se). *Phys. Chem. Chem. Phy.*, vol. *26,* no. 3, pp. 2376-2386, 2024.

[26] J. Ni, L. Yang, and S. Chen, "Effect of transition metal doping on the photoelectric effect of monolayer NbS_2 under strain" First-principles calculations. *Modern Phy. Lett. B*, vol. *38,* no. 04, pp. 01-24, 2024.

[27] H. Dahiya, and K. K. Thakur, "A Review on Synthesis of 2-Dimensional $Mn^{+1}{}_X$ (MXene) materials". In *E3S Web of Conferences*, vol. 309, pp. 01-06, 2021.

[28] S. Kirklin, J. E. Saal, B. Meredig, A. Thompson, J. W. Doak, M. Aykol, and C. Wolverton, "The Open Quantum Materials Database (OQMD): assessing the accuracy of DFT formation energies". *npj Comp. Mat.*, vol. *1,* no. 1, pp. 1-15, 2015.

[29] A. Azizi, M. Dogan, J. D. Cain, K. Lee, X. Yu, W. Shi, and A. Zettl, "Experimental and theoretical study of possible collective electronic states in exfoliable Re-doped NbS_2". *ACS nano*, vol. *15,* no. 11, pp. 18297-18304, 2021.

[30] W. Wang, B. Wang, Z. Gao, G. Tang, W. Lei, X. Zheng, and C. Autieri, "Charge density wave instability and pressure-induced superconductivity in bulk 1 T-NbS_2". *Phys. Rev. B*, vol. *102,* no. 15, pp 115-155, 2020.

[31] F. Güller, C. Helman, and A. M. Llois, "Electronic structure and properties of NbS_2 and TiS_2 low dimensional structures". *Phys. B: Cond. Matt.*, vol. *407,* no. 16, pp. 3188-3191, 2012.

[32] M. Liu, J. Leveillee, S. Lu, J. Yu, H. Kim, C. Tian, and C. K. Shih, "Monolayer 1T-$NbSe_2$ as a 2D-correlated magnetic insulator. *Sci. Adv.*, vol. 9, no. 47, pp. 6339, 2021.